Identification of Rate-Dependent Hysteresis Using the Semilinear Duhem Model*

JinHyoung Oh and Dennis S. Bernstein†

I. Introduction

Hysteresis arises in diverse applications, such as structural mechanics, aerodynamics, and electromagnetics. The word "hysteresis" connotes lag, and hysteretic systems are generally described as having memory. Unlike linear systems and many nonlinear systems, hysteretic systems have the special property that the phase shift between input and output persists even as the frequency content of the input signal approaches DC. Quasi-DC phase shift is the hallmark of hysteresis, and we call a nonlinear system *hysteretic* if it possesses this special property.

With dynamic, that is non-DC, excitation, both linear and nonlinear systems exhibit input-output phase shift, which is generally frequency dependent and a natural consequence of the system's dynamics. Thus, the hysteretic nature of a system is not readily evident from its dynamic response.

However, a special class of hysteretic systems, called *time-scale invariant systems*, have the distinctive property that the input-output phase shift is independent of the time-scaling of the input spectrum. These systems, defined and studied by Chua and Bass [1], are necessarily hysteretic since the quasi-DC phase shift is identical to the phase shift at all frequencies. Because of this rate independence, a plot of the output versus the input is independent of the time scaling of the input and output. Kinematic systems, such as gear backlash, are typically modeled as rate independent.

Roughly speaking, a time-scale invariant system cannot exhibit either resonance or roll-off, which are frequency-dependent phenomena. Of course, the use of linear terminology in this context is merely suggestive of the scale-invariant property of this class of nonlinear systems. The stability of a class of time-scale invariant hysteretic systems was studied in [2].

For hysteretic systems that are not time-scale invariant, the input-output phase shift is frequency dependent. Figure 1 illustrates rate-dependent hysteresis for a simple mass-spring-dashpot system with deadzone [3]. Because of this rate dependence, the hysteretic response near DC is different from the input-output response at higher frequencies. Rate-dependent hysteresis arises commonly in piezoelectric materials [4], [5].

The literature contains a wide variety of hysteresis models, each with the ability to model different features of hysteretic systems. The classical Preisach model [6], [7] is effective for rate-independent hysteresis with complex reversal behavior. Likewise, the Kransnosel'skii–Pokrovskii model [8] has the ability to capture complex reversal mechanisms. In the present paper we focus on the generalized Duhem model, which is based on a nonlinear ordinary differential equation that can model either rate-independent or rate-dependent hysteresis. In the simplest case the generalized Duhem model has the form

$$\dot{x}(t) = f\big(x(t), u(t)\big)g\big(\dot{u}(t)\big), \tag{1}$$

where all variables are scalar and g is continuous and satisfies $g(0) = 0$. Hysteresis arises in the generalized Duhem model (1) when g has a slope discontinuity at the origin. This discontinuity causes the system to exhibit different dynamics whenever u reverses its direction. A special generalized Duhem model, called the *semilinear Duhem model*, was studied in [2]. This system has the form

$$\dot{x}(t) = \big(Ax(t) + Bu(t)\big)g\big(\dot{u}(t)\big). \tag{2}$$

Now assume that g has a slope discontinuity at the origin so that the generalized Duhem model (1) is hysteretic. It turns out that, if g is positively homogeneous, that is, if the graph of g consists of two half-lines emanating from the origin, then the hysteresis is rate-independent, that is, (1) is time-scale invariant. On the other other hand, if g is not positively homogeneous, then the hysteresis is rate dependent.

The generalized Duhem model is also useful for system identification. In [9], the time-scale invariant semilinear Duhem model is used as the basis for system identification. Because of the rate-independence property, the system can be reparameterized in terms of the input signal rather than time. With this reparameterization, the semilinear Duhem model has the form of a linear system with ramp forcing. Consequently, standard least squares techniques can be used for system identification.

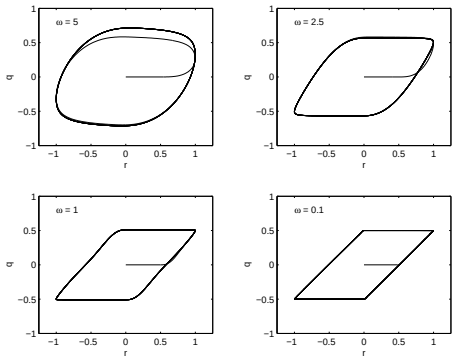

Fig. 1. Frequency-dependent input-output map for a mass-dashpot-spring system with deadzone when $r(t) = \sin \omega t$. Note that phase shift persists near DC, indicating the presence of hysteresis [3].

*This research was supported in part by the National Science Foundation under grant ECS–0225799.

†Department of Aerospace Engineering, The University of Michigan, Ann Arbor, MI 48109-2140, {johzz,dsbaero}@umich.edu

In the case of a rate-dependent system, reparameterization is not possible and the identification problem is much more challenging. Therefore, the goal of the present paper is to develop a technique for identifying systems with rate-dependent hysteresis modeled by the semilinear Duhem model (2). The method we develop exploits a special class of input signals, specifically, triangle waves, which allow the nonlinear function g to be identified in a nonparametric, that is, pointwise, fashion.

II. Generalized Duhem Model and Hysteresis

Consider the single-input single-output *generalized Duhem model* given by

$$\dot{x}(t) = f\big(x(t),u(t)\big)g\big(\dot{u}(t)\big), \quad x(0)=x_0,\ t\geq 0, \tag{3}$$
$$y(t) = h\big(x(t),u(t)\big), \tag{4}$$

where $x : [0,\infty) \to \mathbb{R}^n$ is absolutely continuous, $y : [0,\infty) \to \mathbb{R}$, $u : [0,\infty) \to \mathbb{R}$, $f : \mathbb{R}^n \times \mathbb{R} \to \mathbb{R}^{n\times r}$ is continuous, $g : \mathbb{R} \to \mathbb{R}^r$, and $h : \mathbb{R}^n \times \mathbb{R} \to \mathbb{R}$ is continuous. We assume that g is continuous, piecewise C^1, and satisfies $g(0) = 0$, and we assume that the solution to (3) exists and is unique on all finite intervals. We also assume that h is C^1. Under these assumptions, if u is continuous and piecewise C^1, then x and y are continuous and piecewise C^1. The following definition will be useful.

Definition 2.1:. The nonempty set $\mathcal{H} \subset \mathbb{R}^2$ is a *closed curve* if there exists a continuous, piecewise C^1, and periodic map $\gamma : [0,\infty) \to \mathbb{R}^2$ such that $\gamma([0,\infty)) = \mathcal{H}$.

Definition 2.1 implies that every closed curve is a compact and connected subset of $\mathbb{R}^2$. For closed curves $\mathcal{H}_1$, $\mathcal{H}_2$, define the Hausdorff metric

$$d(\mathcal{H}_1,\mathcal{H}_2) \triangleq \tag{5}$$
$$\max\left\{\sup_{\eta_1\in\mathcal{H}_1}\left(\inf_{\eta_2\in\mathcal{H}_2}\|\eta_1-\eta_2\|\right), \sup_{\eta_2\in\mathcal{H}_2}\left(\inf_{\eta_1\in\mathcal{H}_1}\|\eta_1-\eta_2\|\right)\right\},$$

where $\|\cdot\|$ is a norm in $\mathbb{R}^2$. Since $\mathbb{R}^2$ with $\|x-y\|$ is complete, the set of closed curves with $d(\cdot,\cdot)$ is a complete metric space.

Definition 2.2:. Let $u : [0,\infty) \to [u_{\min},u_{\max}]$ be continuous, piecewise C^1, periodic with period α, and have exactly one local maximum $u_{\max}$ in $[0,\alpha)$ and exactly one local minimum $u_{\min}$ in $[0,\alpha)$. For all $T > 0$, let $u_T(t) \triangleq u(\alpha t/T)$, assume that there exists $x_T : [0,\infty) \to \mathbb{R}^n$ that is periodic with period T and satisfies (3) with $u = u_T$, and let $y_T : [0,\infty) \to \mathbb{R}$ be given by (4) with $x = x_T$ and $u = u_T$. For all $T > 0$, define the *periodic input-output map* $\mathcal{H}_T$ on $[u_{\min},u_{\max}]$ to be the closed curve $\mathcal{H}_T \triangleq \big\{\big(u_T(t),\ y_T(t)\big) : t\in[0,\infty)\big\}$ and assume that the *limiting periodic input-output map* $\mathcal{H}_\infty$ on $[u_{\min},u_{\max}]$ given by $\mathcal{H}_\infty \triangleq \lim_{T\to\infty}\mathcal{H}_T$ exists. If there exist $(u,y_1),\ (u,y_2) \in \mathcal{H}_\infty$ such that $y_1 \neq y_2$, then $\mathcal{H}_\infty$ is a *hysteretic map* on $[u_{\min},u_{\max}]$, and the generalized Duhem model is *hysteretic*.

III. Rate-Independent Semilinear Duhem Model

In this section we characterize the rate-independent generalized Duhem model. The following definition is needed. Note that this definition is independent of the existence of hysteresis.

Definition 3.1:. The generalized Duhem model (3), (4) is *time-scale invariant* if, for all $x(t)$ and $u(t)$ satisfying (3), all initial conditions x_0, and all $T > 0$, it follows that $x_T(t) \triangleq x(t/T)$ and $u_T(t) \triangleq u(t/T)$ also satisfy (3).

The following result is given in [2].

Proposition 3.1:. Assume that g is positively homogeneous, that is, $g(hv) = hg(v)$ for all $h \geq 0$ and $v \in \mathbb{R}$. Then the generalized Duhem model (3), (4) is time-scale invariant.

Suppose that $T > 0$, and let $u(t)$ and $u_T(t)$, where $t \geq 0$, be inputs as in Definition 2.2, and let $x(t)$, $y(t)$, and $x_T(t)$, $y_T(t)$ satisfy the time-scale invariant generalized Duhem model (3), (4) with $u(t)$ and $u_T(t)$, respectively. Suppose there exists a periodic input-output map $\mathcal{H}$ associated with $u(t)$ and $y(t)$. Then the periodic input-output map $\mathcal{H}_T$ associated with $u_T(t)$ and $y_T(t)$ is given by

$$\begin{aligned}\mathcal{H}_T &= \big\{\big(u_T(t),\ y_T(t)\big) : t\in[0,\infty)\big\}\\ &= \big\{\big(u(\alpha t/T),\ h\big(x(\alpha t/T),u(\alpha t/T)\big)\big) : t\in[0,\infty)\big\}\\ &= \big\{\big(u(\alpha t/T),\ y(\alpha t/T)\big) : t\in[0,\infty)\big\}\\ &= \mathcal{H}.\end{aligned}$$

Hence, the periodic input-output map $\mathcal{H}_T$ of the time-scale invariant generalized Duhem model is independent of T, that is, rate independent. Consequently, $\mathcal{H}_T = \mathcal{H}$ for all $T > 0$. Furthermore, if the time-scale invariant generalized Duhem model is hysteretic, then the hysteresis is rate independent.

The following lemma given in [2] is needed to analyze the time-scale invariant generalized Duhem model.

Lemma 3.1:. Assume $g : \mathbb{R} \to \mathbb{R}^r$ is positively homogeneous. Then there exist $h_+ \in \mathbb{R}^r$ and $h_- \in \mathbb{R}^r$ such that

$$g(v) = \begin{cases} vh_+, & v\geq 0,\\ vh_-, & v<0.\end{cases} \tag{6}$$

As a specialization of (3), (4), we consider the *rate-independent semilinear Duhem model*

$$\dot{x}(t) = \big(Ax(t)+Bu(t)\big)g\big(\dot{u}(t)\big), \tag{7}$$
$$y(t) = Cx(t), \qquad x(0)=x_0, \quad t\geq 0, \tag{8}$$

where $A \in \mathbb{R}^{n\times n}$, $B \in \mathbb{R}^n$, and $C \in \mathbb{R}^{1\times n}$, and where $g : \mathbb{R} \to \mathbb{R}$ is positively homogeneous. Note that (7), (8) is the generalized Duhem model (3), (4) with $f(x,u) = Ax+Bu$ and $h(x,u) = Cx$. Since g is positively homogeneous, it follows from Lemma 3.1 that $g\big(\dot{u}(t)\big)$ can be written as

$$g(\dot{u}(t)) = \begin{cases} h_+\dot{u}(t), & \dot{u}(t)\geq 0,\\ h_-\dot{u}(t), & \dot{u}(t)<0,\end{cases} \tag{9}$$

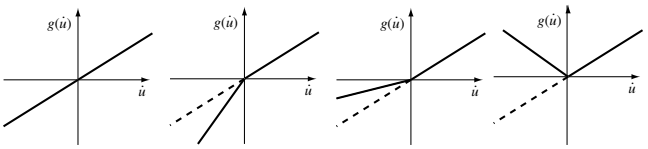

Fig. 2. Illustration of positively homogeneous functions g for asymptotically stable A. (a) not hysteretic, (b) may not converge to $\mathcal{H}_\infty$ since $h_- > h_+$, (c),(d) will converge to $\mathcal{H}_\infty$.

where $h_+ \in \mathbb{R}$ and $h_- \in \mathbb{R}$. The following result given in [2] provides a sufficient condition for (7), (8) to have a limiting periodic input-output map.

Theorem 3.1:. Consider the rate-independent semilinear Duhem model (7), (8), where $u(t) \in [u_{\min}, u_{\max}]$, $t \geq 0$ is piecewise monotonic and periodic with period α and has exactly one local maximum $u_{\max}$ in $[0, \alpha)$ and exactly one local minimum $u_{\min}$ in $[0, \alpha)$. Furthermore, suppose A is asymptotically stable and assume $h_- < h_+$. Then there exists the limiting input-output map $\mathcal{H}_\infty$ on $[u_{\min}, u_{\max}]$ given by

$$\begin{aligned}\mathcal{H}_\infty = &\big\{\big(u, y_+(u)\big) : u \in [u_{\min}, u_{\max}]\big\}\\ &\cup \big\{\big(u, y_-(u)\big) : u \in [u_{\min}, u_{\max}]\big\},\end{aligned} \tag{10}$$

where

$$y_+(u) = Ce^{h_+ A(u-u_{\min})}x_+ + C\mathcal{V}_+(u), \tag{11}$$

$$y_-(u) = Ce^{h_- A(u-u_{\max})}x_- + C\mathcal{V}_-(u), \tag{12}$$

and

$$\hat{x}_+ \triangleq (I - e^{\beta(h_+-h_-)A})^{-1}(e^{-\beta h_- A}\mathcal{V}_+(u_{\max}) + \mathcal{V}_-(u_{\min})), \tag{13}$$

$$\hat{x}_- \triangleq (I - e^{\beta(h_+-h_-)A})^{-1}(e^{\beta h_+ A}\mathcal{V}_-(u_{\min}) + \mathcal{V}_+(u_{\max})), \tag{14}$$

$$\begin{aligned}\mathcal{V}_+(u) \triangleq\ & A^{-1}(uI - u_{\min}e^{h_+A(u-u_{\min})}B + h_+^{-1}A^{-2}\times\\ & (I - e^{h_+A(u-u_{\min})})B,\end{aligned} \tag{15}$$

$$\begin{aligned}\mathcal{V}_-(u) \triangleq\ & A^{-1}(uI - u_{\max}e^{h_-A(u-u_{\max})}B + h_-^{-1}A^{-2}\times\\ & (I - e^{h_-A(u-u_{\max})})B.\end{aligned} \tag{16}$$

Consider the rate-independent semilinear Duhem model (7), (8) and assume that A is asymptotically stable. Then Theorem 3.1 implies that the existence of a limiting periodic input-output map depends on the slopes of g at the origin. Figure 2 illustrates several positively homogeneous functions g. It follows from Theorem 3.1 that for the functions g shown in Figure 2c and Figure 2d the rate-independent semilinear Duhem model has a limiting periodic input-output map.

IV. Rate-Dependent Semilinear Duhem Model

As an alternative specialization of (3) and (4), we consider the *rate-dependent semilinear Duhem model*

$$\dot{x}(t) = \big(Ax(t) + Bu(t)\big)g\big(\dot{u}(t)\big), \tag{17}$$

$$y(t) = Cx(t), \qquad x(0) = x_0, \quad t \geq 0, \tag{18}$$

where $A \in \mathbb{R}^{n\times n}$, $B \in \mathbb{R}^n$, and $C \in \mathbb{R}^{1\times n}$, and where $g : \mathbb{R} \to \mathbb{R}$ is not positively homogeneous. Note that (17), (18) is a generalized Duhem model with $f(x,u) = Ax+Bu$ and $h(x,u) = Cx$. For the following result, let $g'_+(0) \triangleq \lim_{\alpha\downarrow 0}\frac{g(\alpha)}{\alpha}$ and $g'_-(0) \triangleq \lim_{\alpha\uparrow 0}\frac{g(\alpha)}{\alpha}$, where $\lim_{\alpha\downarrow 0}$ and $\lim_{\alpha\uparrow 0}$ denote the right- and left-hand limits at 0.

Corollary 4.1:. Consider the rate-dependent semilinear Duhem model (17), (18) where $u(t) \in [u_{\min}, u_{\max}]$, $t \geq 0$ is piecewise monotonic and periodic with period α and has exactly one local maximum $u_{\max}$ in $[0, \alpha)$ and exactly one local minimum $u_{\min}$ in $[0, \alpha)$. Suppose that A is asymptotically stable, and assume $h_- < h_+$, where $h_+ \triangleq g'_+(0)$ and $h_- \triangleq g'_-(0)$. Then there exists the limiting input-output map $\mathcal{H}_\infty$ on $[u_{\min}, u_{\max}]$ given by (10)–(16).

Proof. Let $T > 0$, and let $u_T(t) \triangleq u(\alpha t/T)$ and linearize (17), (18) with $u = u_T$, $x = x_T$, and $y = y_T$ to obtain the rate-independent semilinear Duhem model

$$\begin{aligned}\Delta\dot{x}_T(t) &= \big(A\Delta x_T(t) + Bu_T(t)\big)g_\Delta\big(\dot{u}_T(t)\big),\\ \Delta y_T(t) &= C\Delta x_T(t), \qquad \Delta x_T(0) = x_0, \quad t \geq 0,\end{aligned}$$

where

$$g_\Delta(\dot{u}_T(t)) \triangleq \begin{cases} h_+\dot{u}_T(t), & \dot{u}_T(t) \geq 0,\\ h_-\dot{u}_T(t), & \dot{u}_T(t) < 0.\end{cases}$$

Then it follows from Theorem 3.1 that the input-output map of $u_T(t)$ and $\Delta y_T(t)$ converges to a closed curve $\mathcal{H}_\infty$ given by (10) as $t \to \infty$. Furthermore, the convergence holds for all $T > 0$ since the model is time-scale invariant. Therefore, it suffices to show that $\|y_T(t) - \Delta y_T(t)\| \to 0$ for all $t \geq 0$ as $T \to \infty$.

For all $T > 0$, let $x_T(t) \in \mathbb{R}^n$, $t \geq 0$, satisfy (17), (18) with $u = u_T$ and $y = y_T$, and define $p_T(t) \triangleq \big(Ax_T(t) + Bu_T(t)\big)\big(g(\dot{u}_T(t)) - g_\Delta(\dot{u}_T(t))\big)$. Since g is piecewise C^1, it follows that

$$\begin{cases}\lim_{\dot{u}_T\downarrow 0}\big(g(\dot{u}_T) - g_\Delta(\dot{u}_T)\big) = 0, & \dot{u}_T \geq 0,\\ \lim_{\dot{u}_T\uparrow 0}\big(g(\dot{u}_T) - g_\Delta(\dot{u}_T)\big) = 0, & \dot{u}_T < 0.\end{cases}$$

Now, for all $T > 0$ and $t \geq 0$, define $e_T(t) \triangleq x_T(t) - \Delta x_T(t)$, satisfies

$$\dot{e}_T(t) = \dot{x}_T(t) - \Delta\dot{x}_T(t) = g_\Delta\big(\dot{u}_T(t)\big)Ae_T(t) + p_T(t), \tag{19}$$

for $e_T(0) = 0$, $t \geq 0$. Let $t_{T,\max} \triangleq \min\{t \geq 0 : u_T(t) = u_{\max}\}$ and $t_{T,\min} \triangleq \min\{t \geq 0 : u_T(t) = u_{\min}\}$. For convenience, assume $t_{T,\max} < t_{T,\min}$. Then, for $q = 0, 1, \ldots$, it follows from (19) that $e_T(t)$ is given by

$$e_T(t) = \begin{cases} \int_0^t \Psi_+(t,\tau)p_T(\tau)\mathrm{d}\tau, & 0 \leq t \leq t_{T,\max},\\ \Psi_-(t, qT + t_{T,\max})e_T(qT + t_{T,\max})\\ \quad + \int_{qT+t_{T,\max}}^t \Psi_-(t,\tau)p_T(\tau)\mathrm{d}\tau,\\ & qT + t_{T,\max} < t \leq qT + t_{T,\min},\\ \Psi_+(t, qT + t_{T,\min})e_T(qT + t_{T,\min})\\ \quad + \int_{qT+t_{T,\min}}^t \Psi_-(t,\tau)p_T(\tau)\mathrm{d}\tau,\\ & qT + t_{T,\min} < t \leq (q+1)T + t_{T,\max},\end{cases}$$

where $\Psi_+(t,\tau) \triangleq \exp h_+\int_\tau^t \dot{u}_T(\sigma)A\mathrm{d}\sigma$ and $\Psi_-(t,\tau) \triangleq \exp h_-\int_\tau^t \dot{u}_T(\sigma)A\mathrm{d}\sigma$. Finally, let $t \geq 0$. Since $\lim_{T\to\infty}$

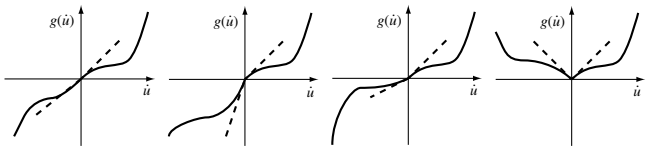

Fig. 3. Illustration of non-positively homogeneous functions g for asymptotically stable A. (a) not hysteretic, (b) may not converge to $\mathcal{H}_\infty$ since $g'_-(0) > g'_+(0)$, (c),(d) will converge to $\mathcal{H}_\infty$.

$|\dot{u}_T(t)| = \lim_{T\to\infty} \alpha|u(\alpha t/T)|/T = 0$, it follows that

$$\lim_{T\to\infty} \Psi_+(t,\tau) = \lim_{T\to\infty} \Psi_-(t,\tau) = I,$$

and $\lim_{T\to\infty} p_T(t) = 0$, and thus $\lim_{T\to\infty} e_T(t) = e_T(0) = 0$. Therefore

$$\lim_{T\to\infty} \|y_T(t) - \Delta y_T(t)\| = \lim_{T\to\infty} \|Cx_T(t) - C\Delta x_T(t)\| \le \|C\| \lim_{T\to\infty} \|e_T(t)\| = 0. \qquad \square$$

Assuming that A is asymptotically stable, Corollary 4.1 implies that the existence of a limiting periodic input-output map for the rate-dependent semilinear Duhem model (17), (18) depends on the slopes of g at the origin. Figure 3 illustrates several non-positively homogeneous functions g. It follows from Corollary 4.1 that for the functions g shown in Figure 3c and Figure 3d the rate-dependent semilinear Duhem model has a limiting periodic input-output map.

V. Rate-Dependent Semilinear Duhem Model with Triangle Wave Inputs

Consider the rate-dependent semilinear Duhem model (17), (18), where $u(t)$ is the periodic triangle wave with period T shown as Figure 4 given by

$$u(t) = \begin{cases} at - aqT - \frac{a}{2}T_a, & qT \le t < qT + T_a, \\ bt - b(q+1)T + \frac{b}{2}T_b, & qT + T_a \le t < (q+1)T, \end{cases} \tag{20}$$

where $a > 0$, $b < 0$, $T_a > 0$, $T_b > 0$, $T = T_a + T_b$, and $q = 0, 1, \ldots$. Then (17), (18) become

$$\dot{x}(t) = \begin{cases} g(a)Ax(t) + g(a)Bu(t), & qT \le t < qT + T_a, \\ g(b)Ax(t) + g(b)Bu(t), & qT + T_a \le t < (q+1)T, \end{cases} \tag{21}$$

$$y(t) = Cx(t), \qquad x(0) = x_0, \quad q = 0, 1, \ldots. \tag{22}$$

Note that (21), (22) can be viewed as a *switching linear time-invariant system* with switching periods T_a and T_b. The following result will be useful.

Proposition 5.1:. Let

$$\dot{x}(t) = Ax(t) + Bu(t), \tag{23}$$

$$y(t) = Cx(t), \qquad x(0) = x_0, \quad t \ge 0, \tag{24}$$

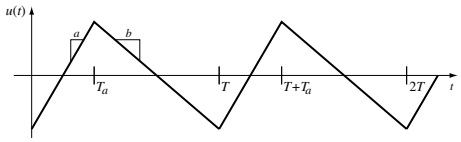

Fig. 4. Triangle wave $u(t)$ defined in (20).

where $A \in \mathbb{R}^{n\times n}$, $B \in \mathbb{R}^n$, $C \in \mathbb{R}^{1\times n}$, be a state-space realization of the linear ordinary differential equation

$$y^{(n)}(t) + \alpha_1 y^{(n-1)}(t) + \cdots + \alpha_{n-1}\dot{y}(t) + \alpha_n y(t) = \beta_1 u^{(n-1)}(t) + \beta_2 u^{(n-2)}(t) + \cdots + \beta_{n-1}\dot{u}(t) + \beta_n u(t), \tag{25}$$

with $\big(y(0), \dot{y}(0), \ldots, y^{(n-1)}(0)\big) = (y_0, y_1, \ldots, y_{n-1})$, $t \ge 0$. Then for $\eta \ne 0$,

$$\dot{x}_\eta(t) = \eta A x_\eta(t) + \eta B u(t), \tag{26}$$

$$y_\eta(t) = Cx_\eta(t), \qquad x_\eta(0) = x_{\eta_0}, \quad t \ge 0, \tag{27}$$

is a state space realization of the linear ordinary differential equation

$$y_\eta^{(n)}(t) + \eta\alpha_1 y_\eta^{(n-1)}(t) + \cdots + \eta^{n-1}\alpha_{n-1}\dot{y}_\eta(t) + \eta^n \alpha_n y_\eta(t) = \eta\beta_1 u^{(n-1)}(t) + \eta^2\beta_2 u^{(n-2)}(t) + \cdots + \eta^{n-1}\beta_{n-1}\dot{u}(t) + \eta^n\beta_n u(t), \tag{28}$$

with $\big(y_\eta(0), \dot{y}_\eta(0), \ldots, y_\eta^{(n-1)}(0)\big) = (y_{\eta_0}, y_{\eta_1}, \ldots, y_{\eta_{n-1}})$, $t \ge 0$.

Proof. Without loss of generality, let A, B, and C be in observable canonical form

$$A = \begin{bmatrix} -\alpha_1 & 1 & \cdots & 0 \\ \vdots & \vdots & \ddots & \vdots \\ -\alpha_{n-1} & 0 & \cdots & 1 \\ -\alpha_n & 0 & \cdots & 0 \end{bmatrix}, \quad B = \begin{bmatrix} \beta_1 \\ \vdots \\ \beta_{n-1} \\ \beta_n \end{bmatrix},$$

$$C = \begin{bmatrix} 1 & 0 & \cdots & 0 \end{bmatrix}.$$

Next, define $T \triangleq \operatorname{diag}(1, \eta^{-1}, \ldots, \eta^{-n+1})$ and note that

$$\eta T^{-1} A T = \begin{bmatrix} -\eta\alpha_1 & 1 & \cdots & 0 \\ \vdots & \vdots & \ddots & \vdots \\ -\eta^{n-1}\alpha_{n-1} & 0 & \cdots & 1 \\ -\eta^n\alpha_n & 0 & \cdots & 0 \end{bmatrix},$$

$$\eta T^{-1} B = \begin{bmatrix} \eta\beta_1 & \cdots & \eta^{n-1}\beta_{n-1} & \eta^n\beta_n \end{bmatrix}^{\mathrm{T}},$$

$$CT = \begin{bmatrix} 1 & 0 & \cdots & 0 \end{bmatrix},$$

which is a realization of (28) $\square$

VI. Identification of the Rate-Dependent Semilinear Duhem Model

Consider the rate-dependent semilinear Duhem model (17), (18), where $u(t)$, $t \ge 0$, is the periodic triangle wave with period T given by (20). Suppose that there exists a periodic solution $x(t)$ of (17), and let $y(t)$, $t \ge 0$, be given by (18). Then it follows from (21), (22) that (17), (18) can be written as

$$\dot{x}(t) = g(a)Ax(t) + g(a)Bu(t), \qquad y(t) = Cx(t), \tag{29}$$

for $0 \le t < T_a$, and

$$\dot{x}(t) = g(b)Ax(t) + g(b)Bu(t), \qquad y(t) = Cx(t), \tag{30}$$

for $T_a \le t < T$. Since (29), (30) is a switching linear time-invariant system, we can identify $g(a)A$, $g(a)B$ on $[0, T_a)$, and $g(b)A$, $g(b)B$ on $[T_a, T)$, where $u(t)$ is monotonically increasing and monotonically decreasing, respectively. Let u_k and y_k, $k = 0, 1, \ldots, l-1$, be measurements of $u(t)$

and $y(t)$, respectively, where $t \in [0, T)$, with a fixed sampling period $h = T/l$. Let $l = l_+ + l_-$, where u_k is monotonically increasing for $k = 0, \ldots, l_+ - 1$ and monotonically decreasing for $k = l_+, \ldots l - 1$.

Next, suppose that u_k and y_k satisfy the n-dimensional DARMA [10, p. 32] model

$$y_{k+1} = -\hat{\alpha}_1^+ y_k - \cdots - \hat{\alpha}_n^+ y_{k-n+1} + \hat{\beta}_1^+ u_k + \cdots + \hat{\beta}_n^+ u_{k-n+1}, \quad (31)$$

for $k = 0, 1, \ldots, l_+ - 1$, and

$$y_{k+1} = -\hat{\alpha}_1^- y_k - \cdots - \hat{\alpha}_n^- y_{k-n+1} + \hat{\beta}_1^- u_k + \cdots + \hat{\beta}_n^- u_{k-n+1}, \quad (32)$$

for $k = l_+, l_+ + 1, \ldots, l - 1$, where $n \leq \frac{l-2}{2}$ is selected empirically, and $\hat{\alpha}_j^+$, $\hat{\alpha}_j^-$, $\hat{\beta}_j^+$, and $\hat{\beta}_j^-$, $j = 1, \ldots, n$ are system parameters. Now, by defining

$$Y_+ \triangleq \begin{bmatrix} y_n & \cdots & y_{l_+-1} \end{bmatrix}^{\mathrm{T}}, \quad Y_- \triangleq \begin{bmatrix} y_{l_++n} & \cdots & y_{l-1} \end{bmatrix}^{\mathrm{T}},$$

$$\Phi_+ \triangleq \begin{bmatrix} -y_{n-1} & \cdots & -y_0 & u_{n-1} & \cdots & u_0 \\ \vdots & \ddots & \vdots & \vdots & \ddots & \vdots \\ -y_{l_+-2} & \cdots & -y_{l_+-n-1} & u_{l_+-2} & \cdots & u_{l_+-n-1} \end{bmatrix},$$

$$\Phi_- \triangleq \begin{bmatrix} -y_{l_++n-1} & \cdots & -y_{l_+} & u_{l_++n-1} & \cdots & u_{l_+} \\ \vdots & \ddots & \vdots & \vdots & \ddots & \vdots \\ -y_{l-2} & \cdots & -y_{l-n-1} & u_{l-2} & \cdots & u_{l-n-1}, \end{bmatrix},$$

least-squares estimates of the system parameters are given by

$$\hat{\theta}_+ = \Phi_+^\dagger Y_+, \qquad \hat{\theta}_- = \Phi_-^\dagger Y_-, \quad (33)$$

where $\hat{\theta}_+ \triangleq \begin{bmatrix} \hat{\alpha}_1^+ & \cdots & \hat{\alpha}_n^+ & \hat{\beta}_1^+ & \cdots \hat{\beta}_n^+ \end{bmatrix}^{\mathrm{T}}$, $\hat{\theta}_- \triangleq \begin{bmatrix} \hat{\alpha}_1^+ & \cdots & \hat{\alpha}_n^+ & \hat{\beta}_1^+ & \cdots \hat{\beta}_n^+ \end{bmatrix}^{\mathrm{T}}$, and $(\ )^\dagger$ denotes the Moore-Penrose generalized inverse.

Next, to obtain coefficients for the continuous time system, we convert the DARMA models (31) and (32) using the bilinear (Tustin) transformation into the continuous time linear ordinary differential equations

$$y^{(n)}(t) + \alpha_1^+ y^{(n-1)}(t) + \cdots + \alpha_n^+ y(t) = \beta_1^+ u^{(n-1)}(t) + \cdots + \beta_n^+ u(t), \quad (34)$$

for $0 \leq t < T_a$, and

$$y^{(n)}(t) + \alpha_1^- y^{(n-1)}(t) + \cdots + \alpha_n^- y(t) = \beta_1^- u^{(n-1)}(t) + \cdots + \beta_n^- u(t), \quad (35)$$

for $T_a \leq t < T$, respectively, where α_j^+, α_j^-, β_j^+, and β_j^-, $j = 1, \ldots, n$, are system parameters. Now, assuming $g(a) \neq 0$, let $g(a) = 1$, which holds without loss of generality by redefining system matrices of (29), (30) by $\hat{A} \triangleq \frac{1}{g(a)} A$ and $\hat{B} \triangleq \frac{1}{g(a)} B$. Then, since (29) is a state-space realization of (34), an estimate of the system matrices in (29) is given by the observable canonical form

$$\hat{A} = \begin{bmatrix} -\alpha_1^+ & 1 & \cdots & 0 \\ \vdots & \vdots & \ddots & \vdots \\ -\alpha_n^+ & 0 & \cdots & 1 \end{bmatrix}, \quad \hat{B} = \begin{bmatrix} \beta_1^+ & \cdots & \beta_n^+ \end{bmatrix}^{\mathrm{T}}, \quad \hat{C} = \begin{bmatrix} 1 & 0 & \cdots & 0 \end{bmatrix}. \quad (36)$$

Furthermore, since (35) can be written in the state space representation (30), Proposition 5.1 implies that (35) and (28) with $\eta = g(b)$, $\alpha_k = \alpha_k^+$ and $\beta_k = \beta_k^+$, $k = 1, \ldots, n$, are equivalent. Comparing coefficients of (35) with those of (28) yields

$$\begin{aligned} &\alpha_1^- = g(b)\alpha_1^+, \quad \alpha_2^- = g^2(b)\alpha_2^+, \quad \cdots \quad \alpha_n^- = g^n(b)\alpha_n^+, \\ &\beta_1^- = g(b)\beta_1^+, \quad \beta_2^- = g^2(b)\beta_2^+, \quad \cdots \quad \beta_n^- = g^n(b)\beta_n^+, \end{aligned} \quad (37)$$

and $g(b)$ is given by the equations involving α_1^+ and β_1^+ as

$$g(b) = \frac{\alpha_1^-}{\alpha_1^+} = \frac{\beta_1^-}{\beta_1^+}. \quad (38)$$

However, (38) is an approximation due to the presence of noise and to the bilinear transformation. An estimate $\hat{g}(b)$ of $g(b)$ is given by the mean value

$$\hat{g}(b) = \frac{\alpha_1^- \beta_1^+ \beta_1^- \alpha_1^+}{2\alpha_1^+ \beta_1^+}. \quad (39)$$

With the system matrices given by (36) and $\hat{g}(b)$ given by (39), we can determine $g(\dot{u})$ pointwise by using same identification procedure involving triangle waves with different slopes. Specifically, let $p \geq 2$ be an integer and, for $i = 1, \ldots, p$, let $u_i(t)$, $t \geq 0$ be a triangle wave input as defined in (20) with periods T_{a_i} and T_{b_i} and slopes $a_i > 0$ and $b_i < 0$. Let $y_i(t)$, $t \geq 0$, be the corresponding steady-state output of the rate-dependent semilinear Duhem model (17), (18), which is periodic with period $T_i = T_{a_i} + T_{b_i}$ so that the input-output map of $u_i(t)$ and $y_i(t)$ forms a closed curve.

Now, for $i = 1, \ldots, p$, identification of the rate-dependent semilinear Duhem model consists of the following steps.

1. Take l_i measurements of $u_i(t)$ and $y_i(t)$ with fixed sampling time h, and then determine the coefficients $\hat{\alpha}_{i_j}^+$, $\hat{\beta}_{i_j}^+$, $\hat{\alpha}_{i_j}^+$ and $\hat{\beta}_{i_j}^+$, $j = 1, \ldots, n$, of the two DARMA models (31), (32) with $\hat{\alpha}_j^+ = \hat{\alpha}_{i_j}^+$, $\hat{\beta}_j^+ = \hat{\beta}_{i_j}^+$, $\hat{\alpha}_j^- = \hat{\alpha}_{i_j}^-$ and $\hat{\beta}_j^- = \hat{\beta}_{i_j}^-$, $j = 1, \ldots, n$.
2. Determine the coefficients $\alpha_{i_j}^+$, $\beta_{i_j}^+$, $\alpha_{i_j}^+$ and $\beta_{i_j}^+$, $j = 1, \ldots, n$, of the linear ordinary differential equations (34), (35) with $\alpha_j^+ = \alpha_{i_j}^+$, $\beta_j^+ = \beta_{i_j}^+$, $\alpha_j^- = \alpha_{i_j}^-$, and $\beta_j^- = \beta_{i_j}^-$, $j = 1, \ldots, n$, by converting the DARMA models from Step 1 to the linear differential equations through the bilinear transformation.

3-1. For $i = 1$, estimate the system matrices $\hat{A}$, $\hat{B}$, and $\hat{C}$ from (36) with $\alpha_j^+ = \alpha_{1_j}^+$, $\beta_j^+ = \beta_{1_j}^+$, $\alpha_j^- = \alpha_{1_j}^-$ and $\beta_j^- = \beta_{1_j}^-$, $j = 1, \ldots, n$. Then set $\hat{g}(a_1) = 1$, and determine $\hat{g}(b_1)$ from (39) with $\alpha_1^+ = \alpha_{1_1}^+$, $\beta_1^+ = \beta_{1_1}^+$, $\alpha_1^- = \alpha_{1_1}^-$, and $\beta_1^- = \beta_{1_1}^-$.

3-2. For determine $\hat{g}(a_i)$ and $\hat{g}(b_i)$ by

$$\hat{g}(a_i) = \frac{\alpha_{i_1}^+ \beta_1^+ + \alpha_1^+ \beta_{i_1}^+}{2\alpha_1^+ \beta_1^+}, \ \hat{g}(b_i) = \frac{\alpha_{i_1}^- \beta_{i_1}^- + \alpha_1^- \beta_{i_1}^-}{2\alpha_1^- \beta_1^-}. \quad (40)$$

VII. Numerical Example

Example 7.1:. Consider the rate-dependent semilinear Duhem model (17), (18) with

$$A = -1, \qquad B = 1, \qquad C = 1, \quad (41)$$

and with the non-positively homogeneous g given by

$$g(v) = \begin{cases} |v|, & |v| \leq 1, \\ 1, & |v| > 1. \end{cases} \quad (42)$$

The identification method developed in Section 6 is used with 12 triangle waves, where $a_i = 0.25, 0.5, 0.75, 1, 1.25,$

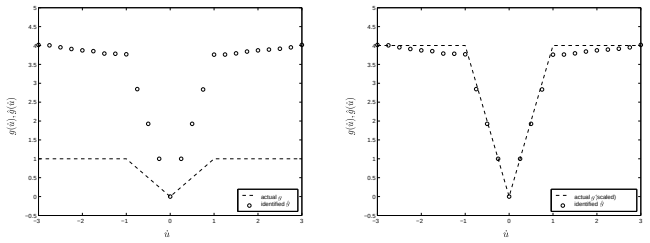

(a) (b)

Fig. 5. (a) actual g (dashed) and pointwise identification $\hat{g}$(circles) of Example 7.1. (b) scaled g (dashed) and $\hat{g}$(circles).

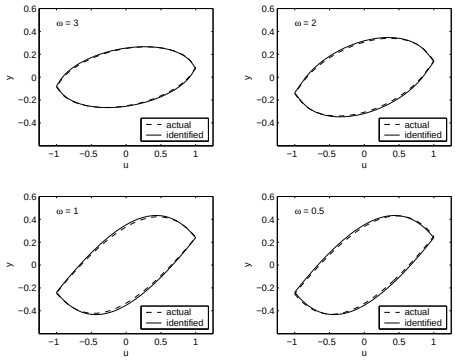

Fig. 6. Input-output maps of actual (dashed) and identified (solid) rate-dependent semilinear Duhem model of Example 7.1 under $u(t) = \sin \omega t$.

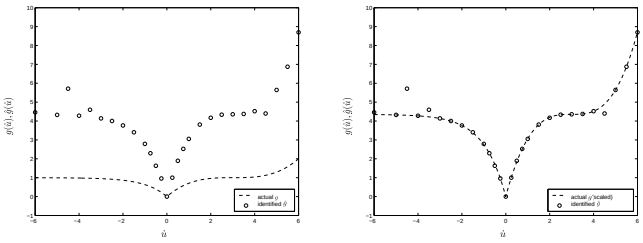

(a) (b)

Fig. 7. (a) actual g (dashed) and pointwise identification $\hat{g}$(circles) of Example 7.2. (b) scaled g (dashed) and $\hat{g}$(circles).

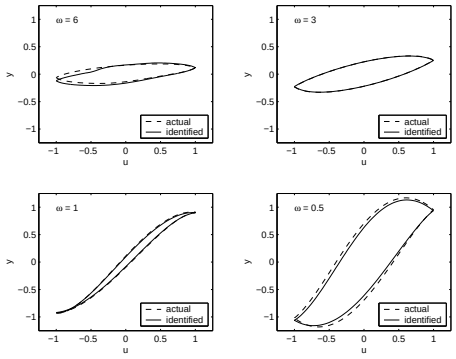

Fig. 8. Input-output maps of actual (dashed) and identified (solid) rate-dependent semilinear Duhem model of Example 7.2 under $u(t) = \sin \omega t$.

$1.5, 1.75, 2, 2.25, 2.5, 2.75, 3$, $b_i = -a_i$, and $T_{a_i} = T_{b_i} = 4/a_i$, $i = 1, \ldots, 12$. Each input u_i and output y_i, $i = 1, \ldots, 12$, were taken with the sampling time $h = 0.13$ second and with a uniformly distributed measurement noise whose range is 1% of the maximum peak-to-peak value over all data. The system parameters are identified as

$$\hat{A} = -0.2501, \qquad \hat{B} = 0.25, \qquad \hat{C} = 1, \qquad (43)$$

and the non-positively homogeneous function $g(\dot{u})$ is identified in pointwise fashion as shown in Figure 5a. Note that the system parameters (43) and identified $\hat{g}$ are scaled by 0.25 and 4, respectively, since $g(a_1) = g(0.25) = 0.25$. Figure 5b shows the scaled graph, which shows that the identified $\hat{g}(\dot{u})$ fits the actual g closely. Figure 6 shows the input-output maps of actual and identified rate-dependent semilinear Duhem model with the identified $\hat{g}$ under sinusoidal inputs.

Example 7.2:. Consider the rate-dependent semilinear Duhem model (17), (18) with

$$A = \begin{bmatrix} 0 & 1 \\ -3 & -1 \end{bmatrix}, \qquad B = \begin{bmatrix} 1 \\ 0 \end{bmatrix}, \qquad C = \begin{bmatrix} 1 & 1 \end{bmatrix}, \quad (44)$$

and non-positively homogeneous g given by

$$g(v) = \begin{cases} \left(\frac{v}{3} - 1\right)^3 + 1, & v \geq 0, \\ 1 - e^v, & v < 0. \end{cases} \qquad (45)$$

For the identification, 14 triangle waves are used with $a_i = 0.25, 0.5, 0.75, 1, 1.5, 2, 2.5, 3, 3.5, 4, 4.5, 5, 5.5, 6$, $b_i = -a_i$, and $T_{a_i} = T_{b_i} = 4/a_i$, $i = 1, \ldots, 14$. The non-positively homogeneous function $g(\dot{u})$ is identified as shown in Figure 7, which shows that the identified $\hat{g}(\dot{u})$ fits the actual g closely for slow inputs. Figure 8 shows the input-output maps of actual and identified rate-dependent semilinear Duhem model with the identified $\hat{g}$ under sinusoid inputs.

REFERENCES

[1] L. O. Chua and S. C. Bass, "A generalized hysteresis model," *IEEE Trans. Circuit Theory*, vol. 19, no. 1, pp. 36–48, 1972.

[2] J. Oh and D. S. Bernstein, "Analysis of the semilinear Duhem model for rate-independent hysteresis," in *Proc. IEEE Conf. Dec. Contr.*, Maui, HI, 2003, to appear.

[3] S. L. Lacy, D. S. Bernstein, and S. P. Bhat, "Hysteretic systems and step-convergent semistability," in *Proc. Amer. Contr. Conf.*, Chicago, IL, June 2000, pp. 4139–4143.

[4] I. D. Mayergoyz, "Dynamic Preisach models of hysteresis," *IEEE Trans. Magnetics*, vol. 24, pp. 2925–2927, 1988.

[5] Y. Yu, Z. Xiao, N. Naganathan, and R. Dukkipati, "Dynamic Preisach modeling of hysteresis for the piezoceramic actuator system," *Mechanism and Machine Theory*, vol. 37, pp. 75–89, 2002.

[6] M. Brokate and A. Visintin, "Properties of the Preisach model for hysteresis," *Journal fur die Reineund Angewandte Mathematik*, vol. 402, pp. 1–40, 1989.

[7] W. Haddad, V. Chellaboina, and J. Oh, "Linear controller analysis and design for systems with input hystereses nonlinearites," *J. Franklin Inst.*, vol. 340, pp. 371–390, 2003.

[8] M. A. Kransnosel'skii and A. V. Pokrovskii, *Systems with Hysteresis*. New York, NY: Springer-Verlag, 1980.

[9] J. Oh and D. S. Bernstein, "Modeling and identification of rate-independent hysteresis using a semilinear Duhem model," in *Proc. 13th IFAC Symposium on System Identification*, Rotterdam, The Netherlands, 2003, pp. 1578–1583.

[10] G. C. Goodwin and K. S. Sin, *Adaptive Filtering Prediction and Control*. Englewood Cliffs, NJ: Prentice-Hall, 1984.